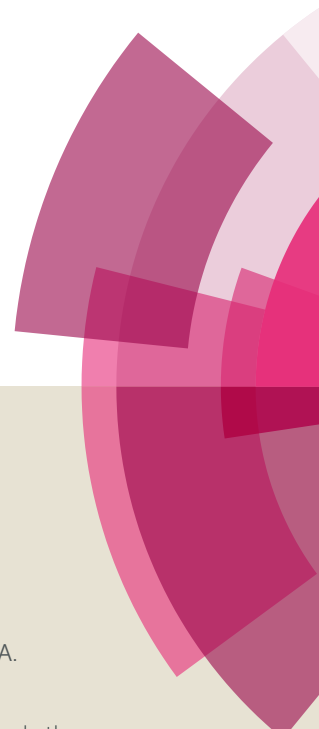


NJC

Accepted Manuscript



This article can be cited before page numbers have been issued, to do this please use: M. M. Hussain, A. M. Asiri, M. N. Arshad and M. M. Rahman, *New J. Chem.*, 2017, DOI: 10.1039/C7NJ01891F.



This is an Accepted Manuscript, which has been through the Royal Society of Chemistry peer review process and has been accepted for publication.

Accepted Manuscripts are published online shortly after acceptance, before technical editing, formatting and proof reading. Using this free service, authors can make their results available to the community, in citable form, before we publish the edited article. We will replace this Accepted Manuscript with the edited and formatted Advance Article as soon as it is available.

You can find more information about Accepted Manuscripts in the [author guidelines](#).

Please note that technical editing may introduce minor changes to the text and/or graphics, which may alter content. The journal's standard [Terms & Conditions](#) and the ethical guidelines, outlined in our [author and reviewer resource centre](#), still apply. In no event shall the Royal Society of Chemistry be held responsible for any errors or omissions in this Accepted Manuscript or any consequences arising from the use of any information it contains.

**Fabrication of Ga³⁺ sensor probe based on
Methoxybenzylidenebenzenesulfonohydrazide (MBBSH) by an
electrochemical approach**

**Mohammad Musarraf Hussain^{a,b}, Abdullah M. Asiri^{a,b}, Muhammad Nadeem Arshad^{a,b},
and Mohammed M. Rahman^{a,b,*}**

^aChemistry Department, Faculty of Science, King Abdulaziz University, Jeddah 21589, P.O. Box 80203, Saudi Arabia. Email: mmrahman@kau.edu.sa, Fax: +966-026952292, Tel: +966-59-6421830.

^bCenter of Excellence for Advanced Material Research, King Abdulaziz University, Jeddah 21589, P.O. Box 80203, Saudi Arabia.

A series of (*E*)-*N'*-methoxybenzylidene-benzenesulfonohydrazide (MBBSH) compounds were synthesized by using a condensation method from the derivatives of methoxybenzaldehyde and benzenesulfonylhydrazine to good crystallized yield in alcoholic medium. The prepared MBBSH compounds were well-characterized by means of various spectroscopic techniques such as ¹H-NMR, ¹³C-NMR, FTIR, and UV-Vis. The structure of the MBBSH molecules were confirmed using a single crystal X-ray diffraction (SCXRD) method and used for the selective detection of the gallium (Ga³⁺) ion by I-V technique. A thin-layer of MBBSH was made by deposition onto a smooth glassy carbon electrode (GCE) with nafion (Nf) as a coating binder in order to modify the sensitive and selective Ga³⁺ sensor probe. Sensitivity, limit of detection

(LOD), and limit of quantification (LOQ) of the modified electrode towards Ga^{3+} were calculated from the calibration curve as $949.37 \text{ pA}\mu\text{M}^{-1}\text{cm}^{-2}$, $\approx 84.0 \pm 0.2 \text{ pM}$, and $280.0 \pm 0.5 \text{ mM}$ respectively. The prospective MBBSH/GCE sensor applied for the determination of Ga^{3+} in spiked biological (Human, mouse, and rabbit serum) and environmental (industrial effluent, red sea water, well-water, and tap water) samples and found acceptable and reasonable results.

1. Introduction

Electrochemical sensors are less expensive, rapid, selective, and sensitive tools used in the research field in heavy metal (HM) detection in quantitatively and qualitatively. Electrochemical signals transduction may be superior to other signal transduction methods in terms of accurateness, selectivity, sensitivity, response time, and stability¹⁻⁷. Gallium (Ga) is a rare element and does not exist in the free form in nature. But Ga^{3+} occurs in nature at trace amounts predominantly in the aluminum matrix, coal, diaspore, germanites, sphalerite, and zinc ores. Gallium is broadly used in electronics and semiconductor industry as a doping element for the production of optoelectronic devices such as laser diodes, light emitting diodes, and transistors. Radioactive Gallium and stable $\text{Ga}(\text{NO}_3)_3$ may be used as a diagnostic and therapeutic agents in bone metabolism, including cancer as well as disorders of calcium. Gallium can be utilized as an anti-tumoral and imaging agent regarding the organ scanning in medicine for the detection of inflammation in patients⁸⁻¹¹. The growing uses of cationic sensor in the area of agricultural, environmental, and medicinal investigation is interesting toward the analytical chemist for the development of a new sensor in terms of accurate, quick, reproducible, and selective detection of different trace elements. In the earlier period, extensive efforts have been given to the advancement of cationic sensor for heavy metal ions (HMI). Among HMI, trivalent

metal ions have acknowledged fewer concentrations in spite of their widespread presence in alloys, animals, foodstuffs, plants, rocks, and fresh including seawater. Various methods such as AAS, AES, calorimetric, chromatography, capillary electrophoretic, electrothermal-AAS, FAAS, fluorimetry, GFAAS, ion-selective electrode, liquid chromatography, mass spectrometry (MS), ICP-AES, ICP-MS, ICP-OES, neutron activation analysis, polarography, spectrometric, UV-Vis spectrophotometry, and X-ray fluorescence spectrometry have been reported for the determination of Ga^{3+} in the earlier studies¹²⁻¹⁵. Other electrochemical methods were also used for the detection of Ga^{3+} , which are presented in Table 3. But these methods are expensive, time consuming and extra care is necessary to perform regarding selective detection of cations. On the other hand, electrochemical cationic sensor is chemically inert, safe, easy to assemble, and invariable in the air^{16,17}.

Gallium has no known physiological role in the human body, but Ga^{3+} is recognized to be highly carcinogenic and toxic for animals as well as humans. So, the detection of Ga^{3+} is important for economic and health purposes¹⁸ in the biomedical aspects. In perspective of the convenience of greatly enhanced selective material, the probability of developing of a particular sensor has opened up a new channel. Our efforts were initiated to develop a sensitive and selective electrode for Ga^{3+} using (*E*)-*N'*-methoxybenzylidene-benzenesulfonylhydrazide (MBBSH) compounds as a sensor substance (Scheme 1). These molecules contain methoxy, imine, and sulfonyl group that have been attracted huge interest as an artificial ionophore due to the binding capacity of HMI with different strength and thus can be a suitable as electro-active material for use in membrane electrodes. The results presented in this article demonstrated that the electrochemical sensor was developed for the determination of Ga^{3+} using MBBSH molecules in an Nf matrix bearing extensive concentration range, short response time, and gives

reproducible results. In our knowledge, this is the first report to detect Ga^{3+} ions using MBBSH derivatives embedded Nf/CGE assembly by I-V approach.

2. Experimental

2.1. Material and methods

The chemicals such as 2-methoxybenzaldehyde, 3-methoxybenzaldehyde, 4-methoxybenzaldehyde, benzenesulfonylhydrazine, AgNO_3 , CdSO_4 , $\text{Co}(\text{NO}_3)_2$, CuSO_4 , $\text{Ga}(\text{NO}_3)_3$, $\text{Pb}(\text{NO}_3)_2$, SbCl_3 , SnCl_2 , $\text{Tl}(\text{NO}_3)_3$, ZnSO_4 , EtOH, NaH_2PO_4 , Na_2HPO_4 , and Nf (5% ethanolic solution) were purchased from the Sigma Aldrich company, Saudi Arabia and used as received. A stock solution of Ga^{3+} (100.0 mM) was made from the purchased salt, $[\text{Ga}(\text{NO}_3)_3]$. Melting point (m. p.) was measured by using a Stuart scientific SMP3 apparatus. ^1H -NMR and ^{13}C -NMR spectra were recorded at 300 K on an AVANCE-III machine (850 and 400 MHz, Bruker, Fallanden, Switzerland), and chemical shifts were reported in ppm by means of orientation with good solvent indication. FTIR spectra were reported as neat on a Thermo scientific NICOLET iS50 FTIR spectrometer. UV-Vis study was carried out using a Evolution 300 UV-Vis spectrophotometer. I-V performance was conducted in order to detect Ga^{3+} at a selective point using the modified 4-MBBSH/GCE by Keithley electrometer (6517A, USA).

2.2. Synthesis of MBBSH molecules

2.2.1. (E)-N'-(2-methoxybenzylidene)benzenesulfonylhydrazide (2-MBBSH, 3): A reaction mixture of benzenesulfonylhydrazine (508.4 mg, 2.95 mmol, and 1.0 equiv) and 2-methoxybenzaldehyde (515.0 mg, 3.78 mmol, and 1.28 equiv) was added in EtOH (20.0 mL), and kept on stirring at R.T. until 3.0 h. Filtered and the obtained white precipitate were washed

with cold EtOH and crystallized from MeOH to give the labeled molecule **3** as a yellowish crystal (433.3 mg, 51.0 %). EF: C₁₄H₁₄N₂O₃S, MW: 290.33, EA: C-57.92, H-4.86, N-9.65, O-16.53, S-11.04. m. p. = 137.9-161.2 °C. ¹H-NMR (400 MHz, DMSO-*d*₆) δ: 11.45 (s, 1H), 8.24 (s, 1H), 7.93-7.86 (m, 2H), 7.71-7.57 (m, 4H), 7.43-7.34 (m, 1H), 7.06 (dd, *J* = 8.5, 1.0 Hz, 1H), 7.01-6.93 (m, 1H), 3.80 (s, 3H). ¹³C-NMR (101 MHz, DMSO-*d*₆) δ: 157.42, 142.68, 139.04, 132.98, 131.64, 129.20, 127.52, 127.10, 125.51, 125.20, 121.55, 120.68, 111.80, 55.64. FTIR (neat) ν_{max}: 3185, 1600, 1495, 1440, 1325, 1275, 1197, 1035, 970, 790, 755, 695, 590. UV-Vis (DMSO, λ_{max}): 322.0 nm.

2.2.2. (E)-N'-(3-methoxybenzylidene)benzenesulfonylhydrazide (3-MBBSH, 4): A reaction combination of benzenesulfonylhydrazine (513.0 mg, 2.98 mmol, and 1.0 equiv) and 3-methoxybenzaldehyde (0.5 mL, 559.0 mg, 4.11 mmol, and 1.38 equiv) was added in EtOH (20.0 mL) and placed on stirring at R.T. After 3.0 h continuous stirring, the resulted solution was filtered and kept at open air to evaporate the solvent. The obtained product was crystallized from EtOH to give the designated molecule **4** as a red crystal (656.5 mg, 76 %). EF: C₁₄H₁₄N₂O₃S, MW: 290.33, EA: C-57.92, H-4.86, N-9.65, O-16.53, S-11.04. ¹H-NMR (850 MHz, DMSO-*d*₆) δ: 11.57 (s, 1H), 7.92-7.88 (m, 3H), 7.66-7.64 (m, 1H), 7.61 (dd, *J* = 8.4, 6.8 Hz, 2H), 7.52-7.50 (m, 1H), 7.13 (dt, *J* = 7.7, 1.2 Hz, 1H), 7.09 (dd, *J* = 2.6, 1.5 Hz, 1H), 6.95 (dd, *J* = 8.4, 2.6 Hz, 1H), 3.74 (s, 3H). ¹³C-NMR (214 MHz, DMSO-*d*₆) δ: 159.87, 147.55, 139.35, 135.40, 133.56, 130.82, 130.40, 129.69, 127.61, 121.44, 119.82, 116.40, 112.00, 55.56. FTIR (neat) ν_{max}: 3200, 2740, 2620, 1725, 1600, 1435, 1315, 1294, 1180, 1035, 900, 800, 770, 700, 600, 510. UV-Vis (DMSO, λ_{max}): 266.4 nm.

2.2.3. (E)-N'-(4-methoxybenzylidene)benzenesulfonohydrazide (4-MBBSH, 5): A reaction mixture of benzenesulfonylhydrazine (506.3 mg, 2.94 mmol, and 1.0 equiv) and 4-methoxybenzaldehyde (0.5 mL, 560.5 mg, 4.12 mmol, and 1.40 equiv) was added in EtOH (25.0 mL), and stirred at R.T. for 3.0 h. The obtained solution was filtered and kept at open air to evaporate the solvent. The found product was crystallized from EtOH to give the designated molecule **5** as a red crystal (838.9 mg, 98 %). EF: C₁₄H₁₄N₂O₃S, MW: 290.33, EA: C-57.92, H-4.86, N-9.65, O-16.53, S-11.04. ¹H-NMR (400 MHz, DMSO-*d*₆) δ: 11.36 (s, 1H), 7.89 (td, *J* = 9.2, 8.6 Hz, 5H), 7.68-7.58 (m, 4H), 7.53-7.48 (m, 1H), 3.86 (s, 3H). ¹³C-NMR (101 MHz, DMSO-*d*₆) δ: 191.35, 164.19, 160.77, 147.30, 138.96, 132.96, 131.81, 129.15, 128.36, 127.15, 126.14, 114.46, 114.21, 55.21. FTIR (neat) ν_{max}: 3198, 1685, 1600, 1500, 1455, 1305, 1275, 1187, 1005, 945, 810, 705, 695, 600, 580, 520. UV-Vis (DMSO, λ_{max}): 274.0 nm.

2.2.4. 4-MBBSH-Ga³⁺ complex (6): A reaction mixture of benzenesulfonylhydrazine (1.0 g, 5.82 mmol, and 2.95 equiv) and 4-methoxybenzaldehyde (1.0 mL, 1.21 g, 8.23 mmol, and 4.18 equiv) was added in EtOH (30.0 mL), and placed on stirring at R.T for 2.30 h. A light white precipitate of 4-MBBSH (**5**) was formed. After that, Ga(NO₃)₃ (500.0 mg, 1.97 mmol, and 1.0 equiv) and EtOH (15.0 mL) were added with **5**, and stirring continued up to 1.5 h at R.T. The obtained product was filtered and precipitate was washed with cold EtOH. The found precipitate was crystallized from MeOH (20 mL) to confer the heading complex (**6**) as a white powder (752.10 mg, 56 %). EF: C₃₀H₃₂GaN₄O₆S₂, MW = 678.45, EA = C-53.11, H-4.75, Ga-10.28, N-8.26, O-14.15, S-9.45. m.p. = 158.5-166.4 °C. ¹H-NMR (400 MHz, DMSO-*d*₆) δ: 11.35 (s, 3H), 8.02-7.81 (m, 9H), 7.72-7.54 (m, 9H), 7.57-7.46 (m, 6H), 7.06-6.86 (m, 6H), 3.77 (s, 9H). ¹³C-NMR (101 MHz, DMSO-*d*₆) δ: 160.78, 147.26, 139.00, 132.96, 129.16, 128.37, 127.16, 126.16,

114.23, 55.23. **FTIR** (neat) ν_{\max} : 3196, 1703, 1600, 1505, 1435, 1308, 1290, 1187, 1100, 1015, 930, 805, 725, 703, 600, 508. **UV-Vis** (DMSO, λ_{\max}): 286.0 nm.

2.3. Crystallography studies of MBBSH molecules

Three new methoxybenzylidene-benzenesulfonohydrazide molecules (**3-5**) were synthesized and crystallized from EtOH at R.T under slow evaporation method. A good looking and grain like crystals were observed in vials. Molecules were screened out under a microscope for good crystals to mount on instrument for data collection. The assembly used to mount samples consists of a glass fiber inserted in the wax and fixed onto the hollow copper tube supported by magnetic base. The specific samples were glued over glass needle and then mounted on Agilent super nova diffractometer and outfitted with micro-focus Cu-Mo $K\alpha$ radiation. The data collection was consummated using CrysAlisPro software at 296 K under the Cu- $K\alpha$ radiation¹⁹. The structures were performed and refined by full matrix least squares technique on F^2 by means of SHELXL-97 ingrained with WinGX²⁰. Non-hydrogen atoms were also distinguished anisotropically by using the same process. The molecular structure of the MBBSH molecules (**3-5**) were generated through PLATON and ORTEP in built with WinGX, and Olex2²¹⁻²⁴. Aromatic carbon and hydrogen atoms were situated geometrically and treated as riding atoms with C-H = 0.93 Å and Uiso (H) = 1.2 Ueq (C) for carbon atoms. N-H atoms were located through Fourier map and distinguished with N-H = 0.84 (2) - 0.86 (2) Å and Uiso (H) = 1.2 Ueq for N atom. Methyl hydrogen atoms were also positioned geometrically and treated as riding atoms with C-H = 0.96 Å and Uiso (H) = 1.5 Ueq (C) for carbon atoms. The disorder for C4 and C5 atoms of aromatic ring has been resolved using constraints in the molecules **3** and **4**. The carbon of methoxy group is also disorder with 75:25 ratios in the same molecules. The Crystal data were

deposited at the Cambridge Crystallographic Data Centre and following deposition numbers have been assigned 1547641 and 1547642 which are known as CCDC number for molecules **3** and **4** respectively. Crystal data may be received without charge on application to CCDC 12 Union Road, Cambridge CB21 EZ, UK.

2.4. Modification of GCE with MBBSH molecules

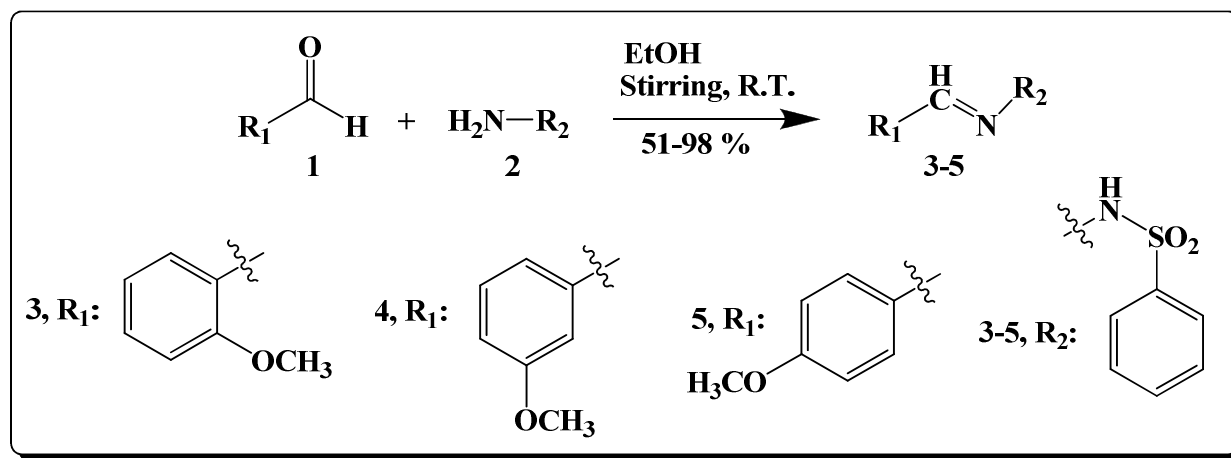
NaH₂PO₄ (93.5, 68.5, 39.0, 16.0, and 5.3 mL), Na₂HPO₄ (6.5, 31.5, 61.0, 84.0, and 94.7 mL), and distilled water, DW (500.0 mL) were taken in order to prepare of a set of phosphate buffer, PB (pH = 5.7, 6.5, 7.0, 7.5, and 8.0) respectively. EtOH and Nf (coating binder) were used to modify the GCE with MBBSH molecules. The GCE were cleaned carefully with DW and acetone subsequently and placed at open air to dry (1.0 h). EtOH was added with MBBSH molecules to make slurry and then deposited on the dried surface of GCE. The deposited electrodes were then kept at open air (2.0 h) for drying. Nf was added in drop wise with the dried deposited electrodes and placed again at open air (1.0 h) for homogeneous film development with complete aeration. The modified GCE and Pt wire were used as working electrode (WE) and counter electrode (CE) successively to record the I-V responses of the desired HMI detection.

3. Results and Discussion

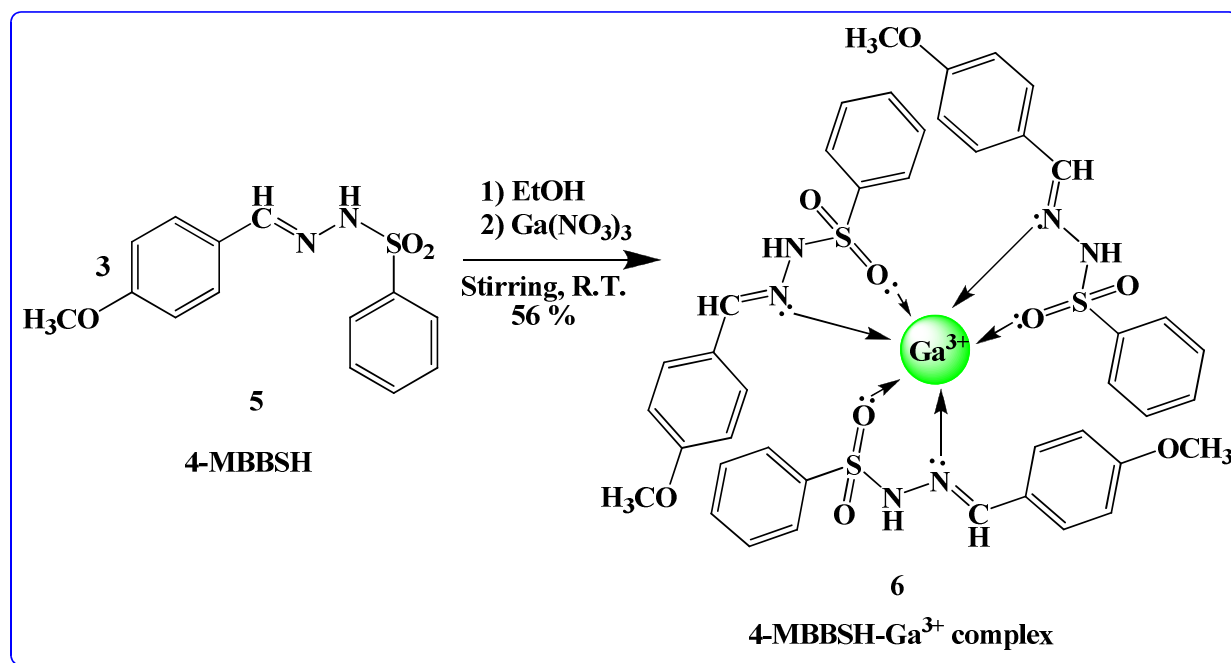
3.1. Spectroscopic studies of MBBSH molecules

The title molecules (**3-5**) were synthesized from 2-methoxybenzaldehyde, 3-methoxybenzaldehyde, 4-methoxybenzaldehyde (**1**), and benzenesulfonylhydrazine (**2**) with

good yield using an easy condensation method (Scheme 1)²⁵. The 4-MBBSH-Ga³⁺ complex (6) was prepared from 4-MBBSH (5) with gallium salt [Ga(NO₃)₃] in a moderate yield (Scheme 2).



Scheme 1 Synthesis of MBBSH molecules



Scheme 2 Synthesis of 4-MBBSH-Ga³⁺ complex

The synthesized compounds 3-5 were characterized using different spectroscopic techniques and finally the structures were recognized using SCXRD examination. The purity of the molecules exhibited good spectra which helped us to classify the existing proton presented in

the compounds using chemical shift (δ) and coupling constant (J). One NH proton of the distinct molecules **3-5** showed singlet at δ 11.45, 11.57, and 11.36 correspondingly. Three N-H proton of the desired molecule **6** showed singlet at δ 11.35. The protons in phenyl groups of the synthesized molecules **3-6** appeared in different signals. Aromatic protons found magnificently at their low field region at δ 6.93-8.24, 6.95-7.92, 7.48-7.89, and 6.68-8.02 respectively for **3-6**. One singlet observed in that order at δ 3.80, 3.74, 3.86, and 3.77 showed three protons for **3-5** and nine protons for **6**, and this may be due to OCH₃. ¹³C-NMR spectra were also recorded and most of the carbon atoms to be found in the aromatic region (†Fig. S1-S8). FTIR spectroscopy were also performed at 4000 – 400 cm⁻¹ for the structure by defining the functional groups *via* diverse bending and stretching peaks found at a particular area in the spectra. UV-Vis spectra were recorded in DMSO respectively (200-800 nm) and the λ_{max} to be reported at 322.0, 266.4, 274.0, and 286.0 nm which is in consequence of the π - π^* shift of the imine functional group (C=NH) in the title molecules **3-6** respectively (†Fig. S9-S12).

3.2. Crystal structure description of MBBSH molecules

The arrangements of molecule in crystal system and the interactions between them affect the physico-chemical properties of synthesized compounds. The efforts of crystallization were performed to observe three-dimensional arrangements and interactions of molecules. The compound **3** and **4** were crystallized in triclinic and monoclinic crystal system with P-1 and P2₁/c space group respectively (Table 1). Compound **3** occupied two independent molecules in an asymmetric unit cell. It is already observed that S atom in sulfonamides adopted distorted tetrahedral geometry so the pattern was observed here with $\angle\text{O1-S1-O2} = 119.06$ (8) °, $\angle\text{O4-S1-O5} = 119.31$ (8) °, and $\angle\text{O1-S1-O2} = 119.23$ (12) ° for molecules **3** and **4** correspondingly²⁶⁻²⁹

(†Table S1 and S2). All other angles around S atoms are $\leq 110^\circ$. In molecule **3a**, both of the aromatic rings are perpendicular to each other with the dihedral angle of $89.67(5)^\circ$, while in **3b**, this angle is short by almost ten degrees i.e. $80.82(2)^\circ$. The compound **4** has disorder in aromatic ring and methoxy group (Fig. 1). Molecule **3a** affords only intermolecular hydrogen bonding and gives rise to the formation of dimmers $R_2^2(8)$, while **3b** extends the formation of dimmers via C-H...O interaction along *b*-axis in zig-zag manners³⁰. In compound **4**, the interactions give rise to the formation of supra molecule along in three dimensions. The $N_2-H_2N...O_1$, $C_4-H_4...O_2$, and $C_{12}-H_{12}...O_2$ were connected along *a*-axis, *b*-axis, and *c*-axis respectively in the molecules **3** and **4** (Fig. 2 and Table 2). The crystal structure of the molecule **5** has been confirmed with the previously published data³¹.

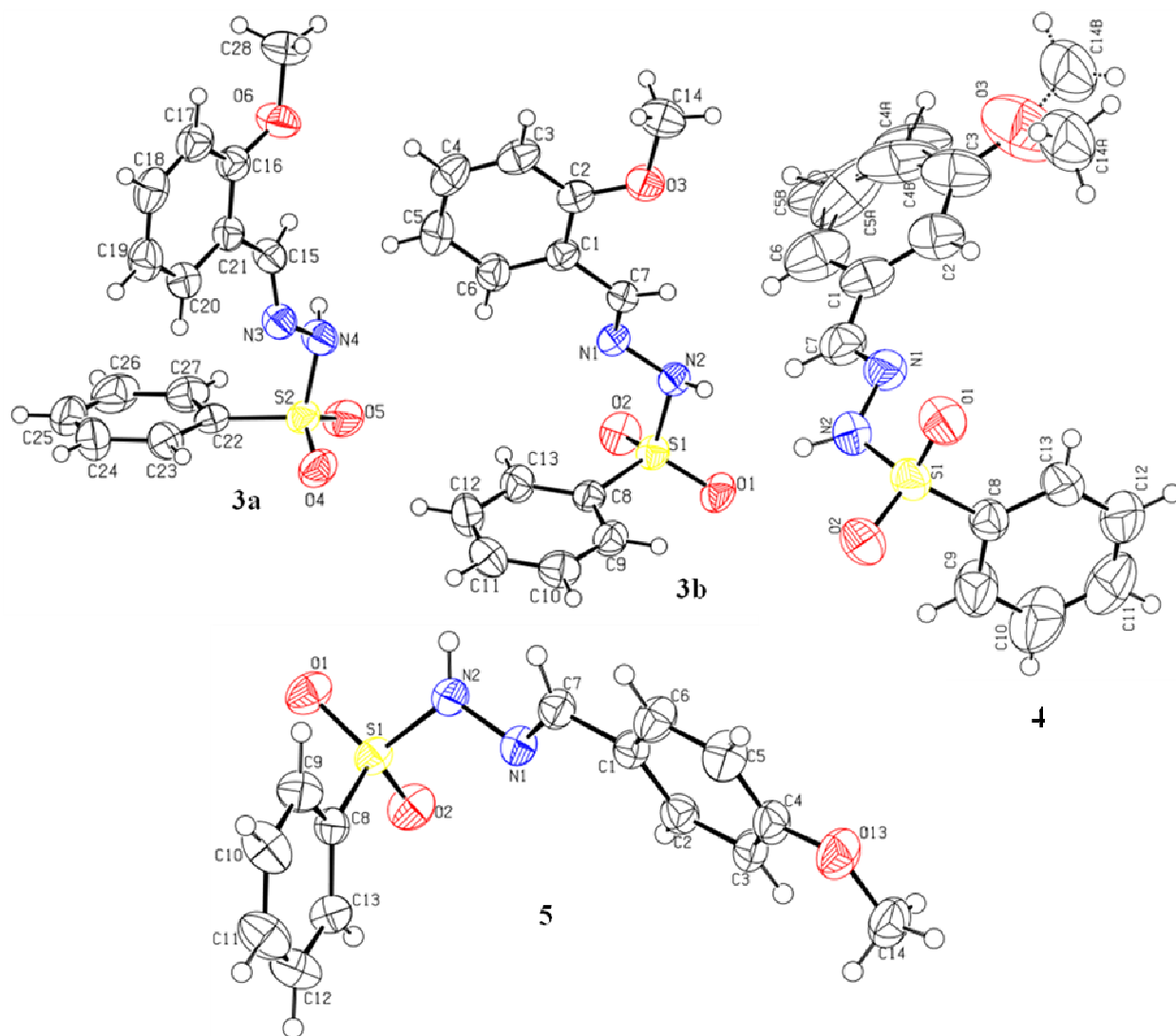


Fig. 1 Molecular structure of MBBSH molecules

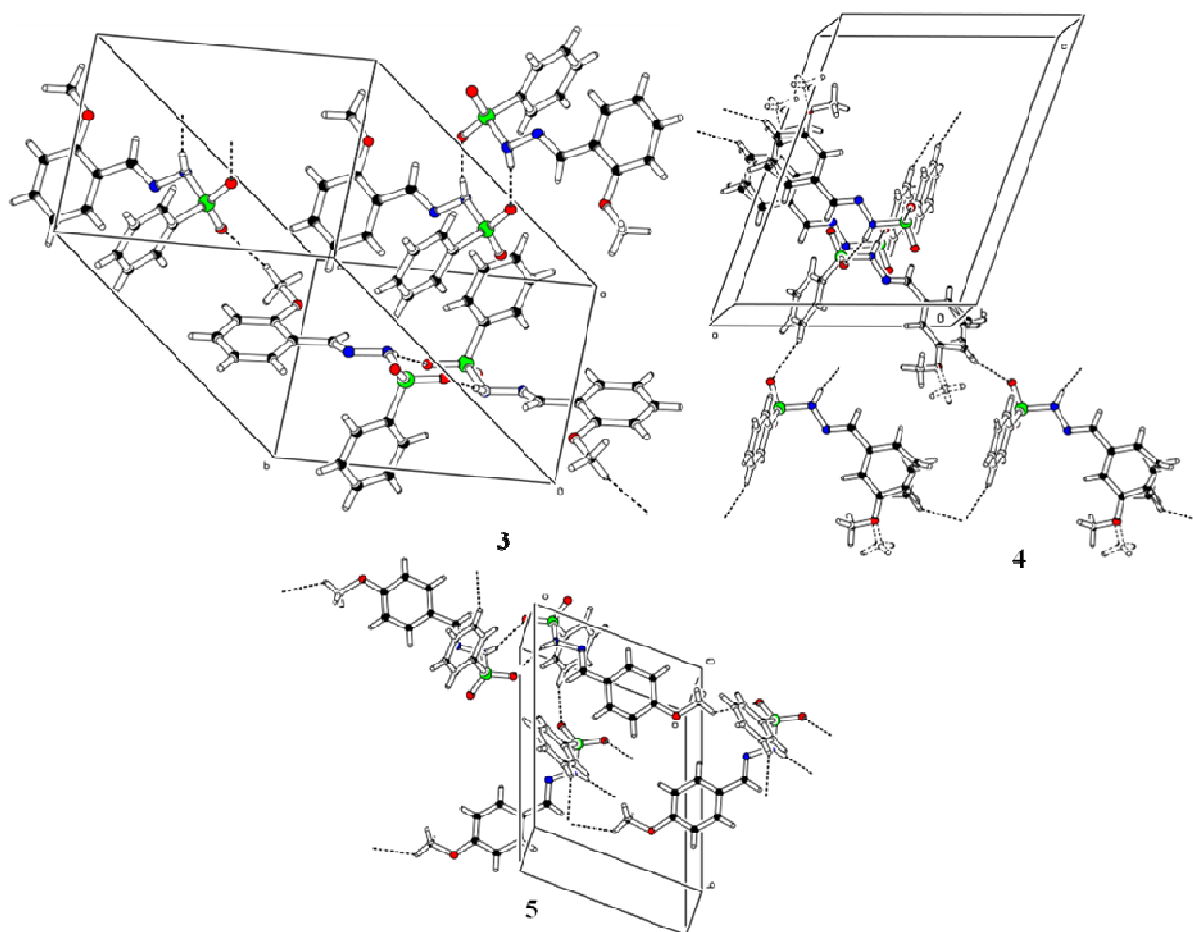


Fig. 2 Hydrogen bonding pattern of MBBSH molecules

Table 1 Crystal data and structure refinement for MBBSH molecules

Parameters	MBBSH	
	3	4
ID Number	16155	17030
CCDC Number	1547641	1547642
Empirical formula	C ₁₄ H ₁₄ N ₂ O ₃ S	C ₁₄ H ₁₄ N ₂ O ₃ S
Formula weight	290.33	290.33
Temperature/K	296 (2)	296 (2)
Crystal system	triclinic	monoclinic
Space group	P-1	P2 ₁ /c
a/Å	8.8094 (5)	12.1076 (9)
b/Å	11.2917 (8)	8.0030 (4)
c/Å	14.9528 (9)	15.9338 (13)
α/°	73.214 (5)	90
β/°	85.325 (4)	110.860 (9)

$\gamma/^\circ$	83.268 (5)	90
Volume/ \AA^3	1412.43 (16)	1442.74 (19)
Z	4	4
$\rho_{\text{calc}} \text{ mg/mm}^3$	1.365	1.337
μ/mm^{-1}	0.237	0.232
F(000)	608.0	608.0
Crystal size/ mm^3	$0.48 \times 0.46 \times 0.32$	$0.48 \times 0.46 \times 0.32$
2 θ range for data collection	5.886 to 58.42 $^\circ$	7.204 to 57.988 $^\circ$
Index ranges	$-11 \leq h \leq 12, -11 \leq k \leq 14, -20 \leq l \leq 20$	$-16 \leq h \leq 14, -9 \leq k \leq 10, -21 \leq l \leq 16$
Reflections collected	12804	6926
Independent reflections	6701 [R(int) = 0.0192]	3416 [R(int) = 0.0269]
Data/restraints/parameters	6701/2/367	3416/12/190
Goodness-of-fit on F ²	0.963	0.865
Final R indexes [$I \geq 2\sigma(I)$]	$R_1 = 0.0410$ and $wR_2 = 0.1098$	$R_1 = 0.0538$ and $wR_2 = 0.1417$
Final R indexes [all data]	$R_1 = 0.0529$ and $wR_2 = 0.1222$	$R_1 = 0.0783$ and $wR_2 = 0.1697$
Largest diff. peak/hole / $e \text{ \AA}^{-3}$	0.20/-0.49	0.35/-0.39
Flack parameter	---	---

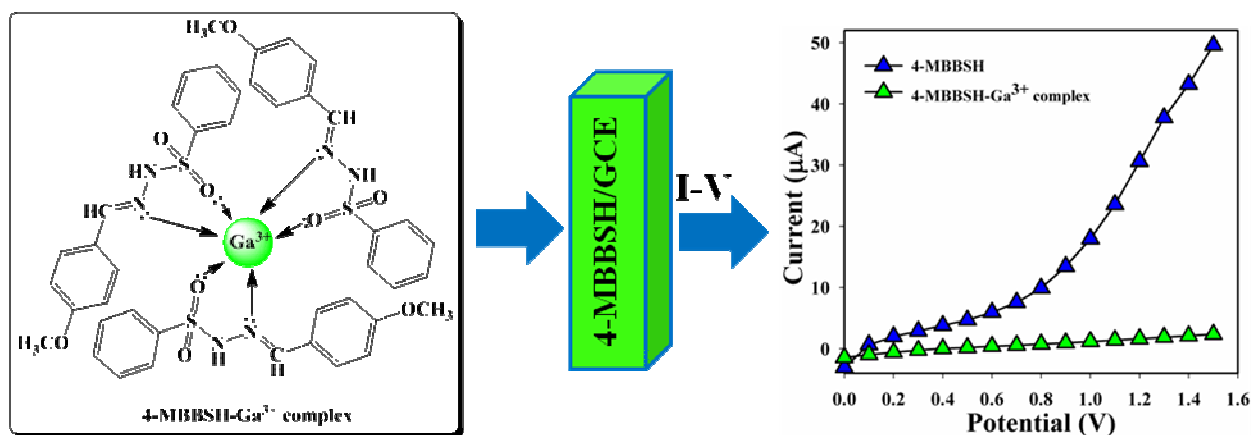
Table 2. Hydrogen Bonds for MBBSH molecules

MBBSH	D	H	A	d(D-H)/ \AA	d(H-A)/ \AA	d(D-A)/ \AA	D-H-A/ $^\circ$
3	C34	H34B	O2 ¹	0.96	2.47	3.419 (3)	168.7
	N2	H1	O1 ²	0.854 (16)	2.059 (17)	2.9073 (19)	172 (2)
	N4	H2	O5 ³	0.837 (16)	2.095 (17)	2.915 (2)	166 (3)
¹ 1-X,-Y,1-Z; ² 2-X,-Y,1-Z; ³ 1-X,1-Y,2-Z							
4	C12	H12	O2 ¹	0.93	2.59	3.362 (4)	141.2
	C13	H13	O1 ²	0.93	3.05	3.534 (3)	114.5
	N2	H2A	O1 ³	0.86	2.39	3.075 (3)	137.4
¹ +X,1/2-Y,-1/2+Z; ² 1-X,-Y,1-Z; ³ 1-X,1/2+Y,3/2-Z							

4. Application

4.1. Detection of Gallium(III) ion by Methoxybenzylidene-benzenesulfonylhydrazide compounds

Development of the modified electrode (ME) with small organic molecule is the beginning phase of application as a HMI sensor. The 4-MBBSH fabricated GCE was examined in PB for the detection of desired HMI, Ga^{3+} . The proposed 4-MBBSH/GCE sensor was demonstrated a diversity of advantages such as chemically not active, simple to construct, not dangerous, simple to assemble, and constant in air. Based on the I-V theory, current signals of the 4-MBBSH/GCE sensor extensively changed throughout the adsorption of Ga^{3+} by means of electrochemical approach. The proposed mechanism of 4-MBBSH- Ga^{3+} complex arrangement^{32,33} and comparison I-V response between 4-MBBSH and 4-MBBSH- Ga^{3+} complex using proposed sensor, 4-MBBSH/GCE is presented in **Scheme 3**.



Scheme 3 Comparison of I-V responses between 4-MBBSH and 4-MBBSH- Ga^{3+} complex using proposed sensor, 4-MBBSH/GCE.

The broad application of MBBSH adapted electrode as a HMI sensor was the finding of preferred cation that are not as much of precious in natural region. At the commencement, pH of the different PB was examined in perspective of 2-MBBSH to find out which system was more

appropriate to identify the desired HMI as well as pH = 7.5, which appeared more response towards the ME compared with other PB (Fig. 3a). Subsequently, derivatives of MBBSH were optimized in PB (pH = 7.5) and 4-MBBSH showed prime responses (Fig. 3b), where bar diagram of MBBSH optimization at +1.2 V with error limits (EL) 10.0 % is presented in Fig. 3c. I-V responses for the bare GCE, GCE with coating binder and coated with 4-MBBSH on the WE were presented in Fig. 3d, where the differentiation of the current signals among the electrodes happened due to responses were augmented by the layered GCE in compared with bare and GCE with Nf.

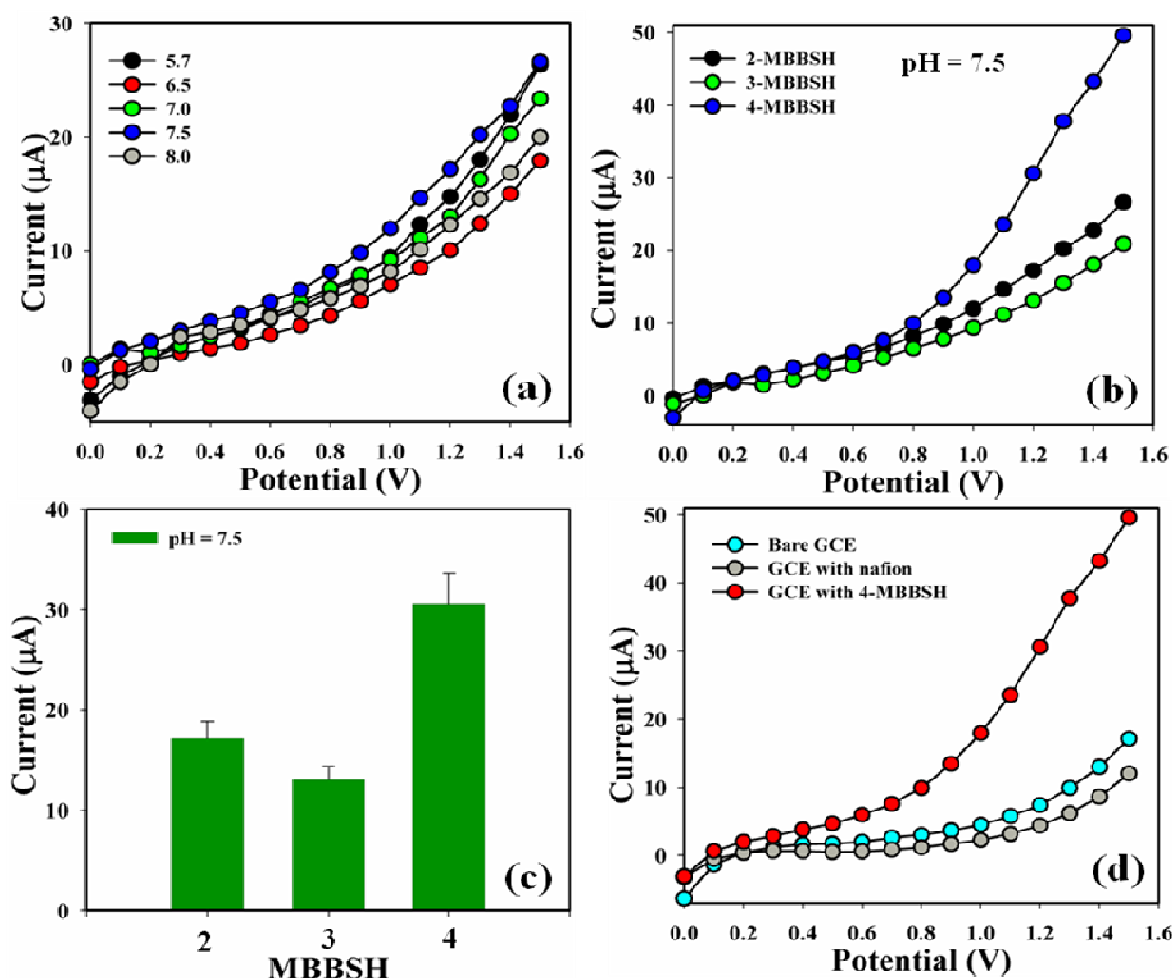


Fig. 3 (a) pH examination, (b) MBBSH molecules optimization at pH = 7.5, (c) Bar diagram presentation of MBBSH optimization at +1.2 V with EL 10.0 %, and (d) Bare and coated electrode.

The HMI such as Ag^+ , Cd^{2+} , Co^{2+} , Cu^{2+} , Ga^{3+} , Pb^{2+} , Sb^{3+} , Sn^{2+} , Tl^{3+} , and Zn^{2+} were investigated at $1.0 \mu\text{M}$ in order to find out the maximum responses towards 4-MBBSH ME and accordingly it was noticeably observed that the sensor was more discerning towards Ga^{3+} in comparison with other ions (Fig. 4a). The selectivity was optimized at $1.0 \mu\text{M}$ in perspective of MBBSH molecules and 4-MBBSH showed major responses to Ga^{3+} (Fig. 4b). Fig. 4c is the bar diagram presentation of selectivity optimization at + 1.2 V with EL 10.0 %. The current responses (CR) without Ga^{3+} (black-dotted) and with Ga^{3+} (green, grey, and red dotted) were also examined (Fig. 4d). An increase of CR originated relating to the 4-MBBSH tailored electrode with Ga^{3+} , which has been given a massive exterior arena with superior exposure in incorporation and adsorption effectiveness onto the permeable 4-MBBSH surfaces to the favored HMI.

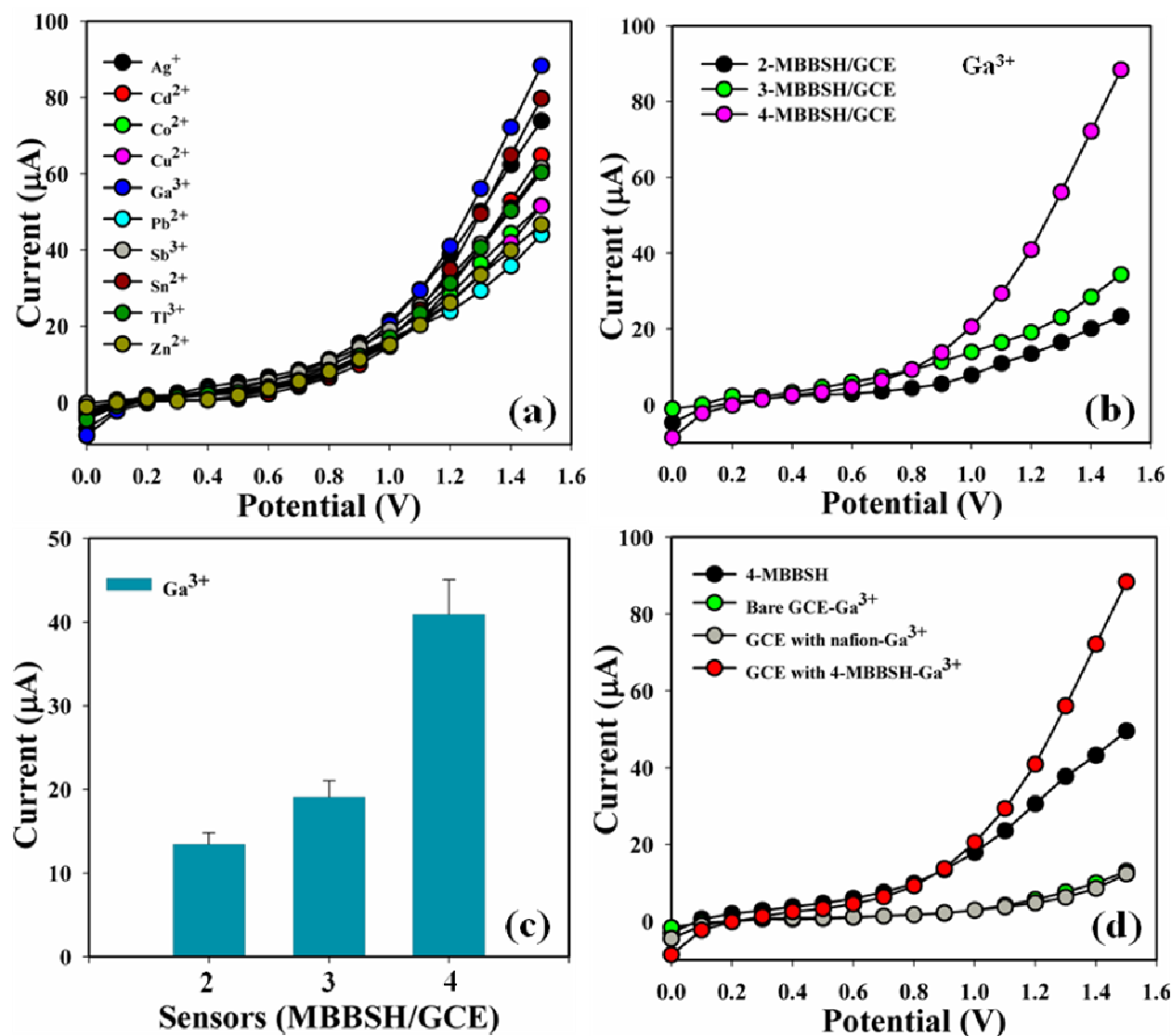


Fig. 4 (a) Selectivity study at $1.0 \mu\text{M}$, (b) Selectivity optimization towards Ga^{3+} in perspective of MBBSH molecules ($1.0 \mu\text{M}$), (c) Bar diagram presentation of selectivity optimization at +1.2 V with EL 10.0 %, and (d) I-V responses in absence and presence of Ga^{3+} .

The CR of the Ga^{3+} with diverse concentration ($100.0 \text{ pM} \sim 100.0 \text{ mM}$) towards 4-MBBSH ME were investigated with indication of the changes of current of the custom-made electrode is a purpose of Ga^{3+} recognition under regular array. It was found that the CR augmented on a regular basis from lower to higher concentration of the desired HMI (Ga^{3+}), [SD

= 0.84, RSD = 41.33 % at + 0.5 V, and n = 10] (Fig. 5a). A good series of the Ga³⁺ concentrations were investigated from the lower to higher potential (0.0 ~ + 1.5 V) in progression to find out the feasible methodical perimeter. The calibration curvature (CC) was plotted at + 0.5 V from Ga³⁺ concentration range (100.0 pM ~ 100.0 mM) and found linear [$R^2 = 0.9486$, SD = 0.84, n = 10, and EL 10.0 %] (Fig. 5b). Sensitivity, LOD, and LOQ were calculated using the equation (i-iii)^{34, 35} and found as $949.37 \text{ pA}\mu\text{M}^{-1}\text{cm}^{-2}$, $\approx 84.0 \pm 0.2 \text{ pM}$, and $280.0 \pm 0.5 \text{ mM}$ respectively. Where, m = slope of the CC, A = active surface area of GCE ($\sim 0.0316 \text{ cm}^2$), and SD = standard deviation of Ga³⁺ concentration at the calibrated potential, CP (+ 0.5 V). LDR (100.0 pM ~ 1.0 mM) was also considered from the CC and found linear, $R^2 = 0.9531$ (Fig. 5c). Response time (r. t.) of Ga³⁺ towards 4-MBBSH/GCE sensor was measured at 1.0 μM and found 7.0 s (Fig. 5d).

$$\text{Sensitivity} = \frac{m}{A} \quad (i)$$

$$\text{LOD} = \frac{(3 \times \text{SD})}{m} \quad (ii)$$

$$\text{LOQ} = \frac{(10 \times \text{SD})}{m} \quad (iii)$$

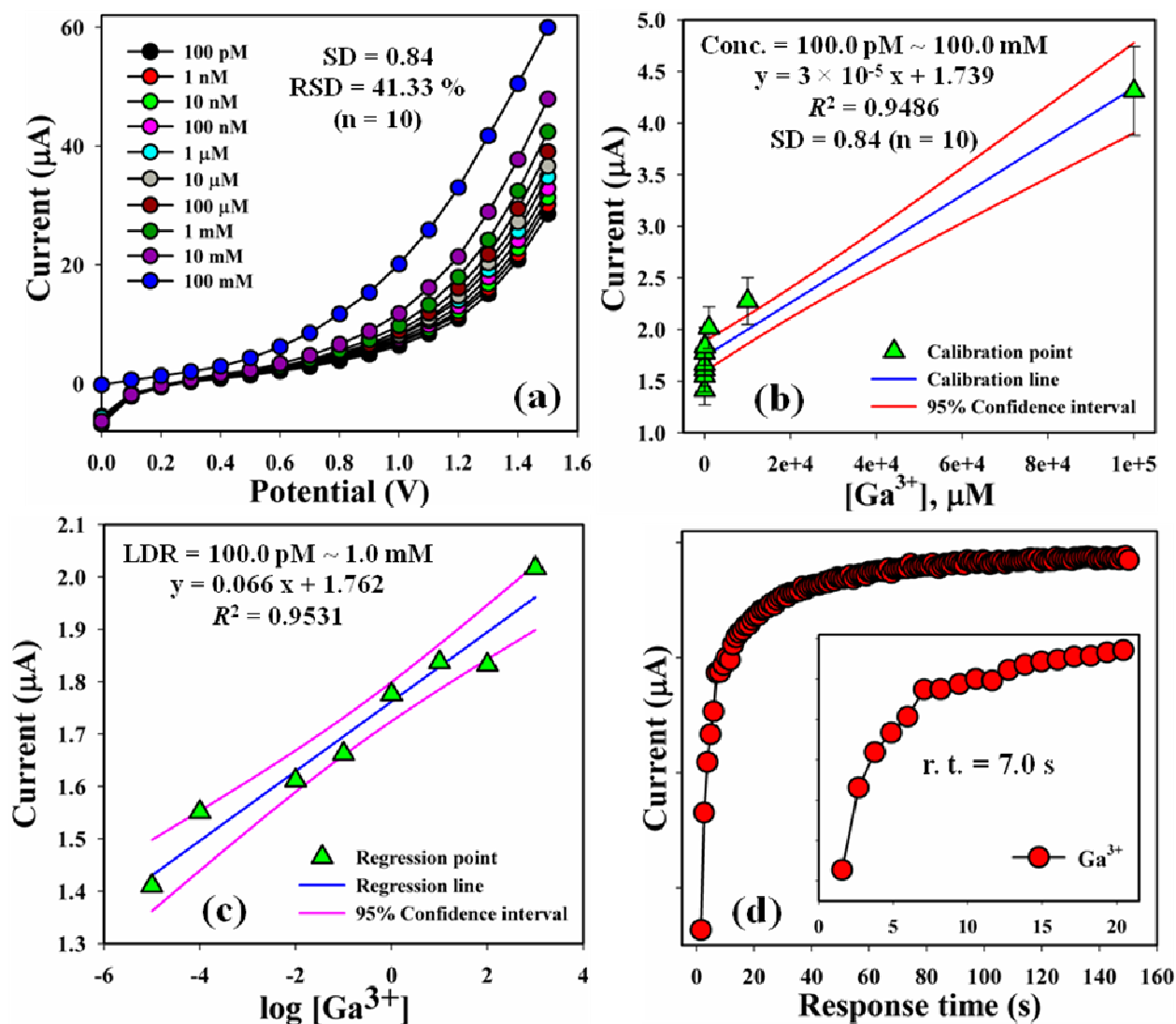


Fig. 5 (a) Concentration variation examination, (b) Calibration curve at +0.5 V with EL 10.0 %, (c) LDR plot, and (d) Response time of Ga^{3+} towards 4-MBBSH/GCE sensor.

4.2. Sensor potentiality examination

The sensing potentiality of the 4-MBBSH/GCE sensor was examined up to few days in order to estimate of the reproducible (RP) capabilities. Consequently, a series of six consecutive degree of Ga^{3+} at 1.0 μM ($\sim 25.0 \mu\text{L}$) was conducted using different ME at room condition and yielded good RP responses (RP = 72 %, SD = 0.47, RSD = 23.21 %, and n = 6) towards the 4-MBBSH/GCE sensor (Fig. 6a and †Table S3). It was acknowledged that the I-V responses were

not comprehensively changed after cleaning of each trial of the modified 4-MBBSH electrode. The sensitivity remained almost similar the unusual responses up too few days and after that the responses of the ME become declined continually. The responses of the 4-MBBSH sensor were considered with admiration to storage time for the intention of elongated storage susceptibility. The gratitude of storage propensity of the 4-MBBSH/GCE sensor was evaluated and in this regards a progression of six successive replicates of Ga^{3+} at $1.0 \mu\text{M}$ ($\sim 25.0 \mu\text{L}$) was examined under standard arrangement using same ME. The repeatability (RA) of the proposed sensor at CP ($+ 0.5 \text{ V}$) was found 87.0 % towards Ga^{3+} , [SD = 0.12, RSD = 8.99 %, and $n = 6$] (Fig. 6b and †Table S3). It was noticeably reported that the expected sensor can be used devoid of any major fall down of sensitivity up to few days. By using different ME, a comparison of Ga^{3+} recognition is presented in Table 3. Where, analytical (i.e. sensing) parameters were not determined in detailed in the previous studies. But, in our research, sensitivity including other parameters such as LOD and LDR of the proposed sensor (4-MBBSH/GCE) were determined with good results.

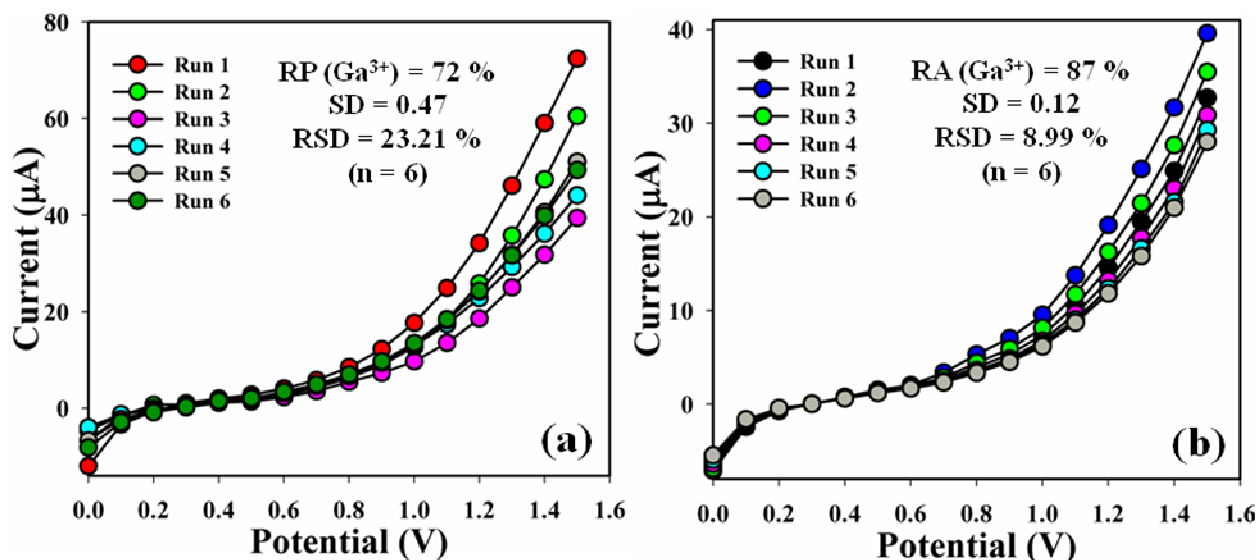


Fig. 6 (a) Reproducible and (b) Repeatability study of the proposed 4-MBBSH/GCE sensor.

Table 3. Determination of Ga³⁺ using different modified electrodes

Methods	Modified electrodes	Sensitivity	LOD (µg/L)	LDR (µg/L)	Ref
SWASV	BiFE	---	2.3	20-100	36
Spectrophotometry	---	---	14	46.9-2.24 (µg/L-mg/L)	37
Spectrofluorimetry	---	---	2	3-30	38
Spectrofluorimetry	---	---	0.5	40-80	39
Chromatography	---	---	---	5-100 mg/L	40
AAS	---	---	0.29 ng/L	0-80 ng/L	41
AES	---	---	---	0.5-500 mg/L	42
NAA	---	---	0.5	0-10	43
ICP-MS	---	---	0.02 ppt	2-60 pM	44
ICP-MS	---	---	60 ng/L	0.2-100	45
ASV	Mercury	---	~25 ng/L	0.09-40	46
Voltammetry	MFSBE	---	7 ng/L	0.14-6.97	47
Potentiometry	CNCCPE	---	36.4	55.3-2.24 (µg/L – g/L)	48
I-V	4-MBBSH/GCE	949.37 pAµM ⁻¹ cm ⁻²	84.0 ± 0.2 pM	100.0 ~ 1.0 (pM ~ mM)	This work

SWASV: Square wave anodic stripping voltammetry, BiFE: bismuth film electrode, AAS: Atomic absorption spectrometry, AES: Atomic emission spectrometry, NAA: Neutron activation analysis, ASV: Anodic stripping voltammetry, MFSBE: Mercury film silver based electrode, CNCCPE: Carbon nanotube composite coated platinum electrode, and I-V: Current-voltage.

4.3. Prospective examination of interference effect (IEF)

Examination of IEF is one of the considerable practices in analytical science having the potential in order to make difference of the interfering agents (IA) from the HMI bearing similar cationic nature. Al^{3+} , Ba^{2+} , Ca^{2+} , K^+ , and Na^+ are generally used as IA in the electrochemical Ga^{3+} revealing⁴⁹. I-V responses at 4-MBBSH/GCE sensor toward the addition of Ga^{3+} ($1.0 \mu\text{M}$ and $\sim 25.0 \mu\text{L}$) and IA such as Al^{3+} , Ba^{2+} , Ca^{2+} , K^+ , and Na^+ ($10.0 \mu\text{M}$ and $\sim 25.0 \mu\text{L}$) in PB (pH = 7.5) were examined using similar ME. The IEF of IA towards Ga^{3+} was calculated at the CP (+ 0.5 V), where the IEF of Ga^{3+} was considered to be 100.0 % (Fig. 7a-b and Table 4). It was noticeable that 4-MBBSH/GCE sensor did not show any remarkable responses towards the IA. So, the proposed sensor is suitable for the detection of Ga^{3+} with good sensitivity.

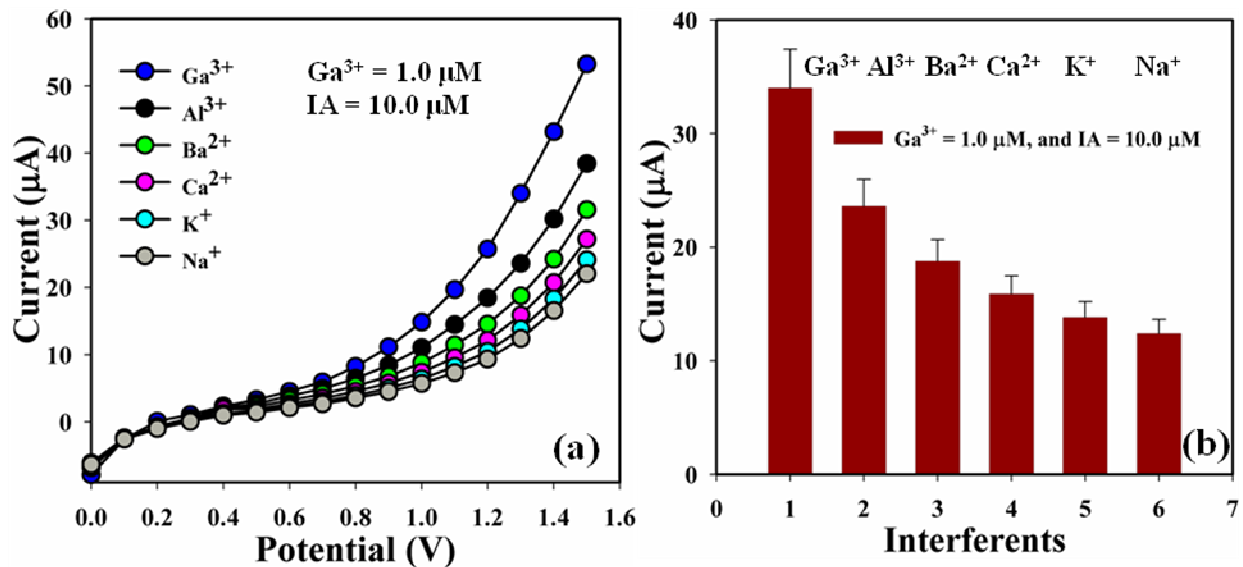


Fig. 7 (a) IEF study and (b) Bar diagram presentation of IEF at + 1.3 V with EL 10.0 %.

Table 4. Interference effect examination of heavy metal ions towards Ga^{3+}

Interfering agents	Current (μA)				Interference effect (%)	SD (n = 3)	RSD (%) (n = 3)
	R1	R2	R3	Average			
Ga^{3+}	4.39	2.89	2.64	3.31	100	0.95	28.62
Al^{3+}	3.13	2.74	2.37	2.75	83	0.38	13.84
Ba^{2+}	2.72	2.12	2.12	2.32	70	0.35	14.93
Ca^{2+}	2.14	1.70	1.85	1.89	57	0.22	11.79
K^+	1.95	1.43	1.47	1.62	49	0.29	17.90
Na^+	1.79	1.28	1.21	1.43	43	0.32	22.19

5. Analysis of real samples

A set of real samples (RS) such as human serum (HS), mouse serum (MS), rabbit serum (RaS), industrial effluent (IE), red sea water (RSW), well water (WW), and tap water (TW) were examined in order to sustain of the expected I-V performance using 4-MBBSH/GCE sensor. A usual addition process was used to find out the concentration of Ga^{3+} in RS. A set quantity ($\sim 25.0 \mu\text{L}$) of all RS was examined in PB (10.0 mL, 100.0 mM, and $\text{pH} = 7.5$) using the modified 4-MBBSH/GCE sensor. The concentrations were calculated at the CP (+ 0.5 V) regarding the detection of Ga^{3+} in HS, MS, RaS, IE, RSW, WW, and TW which perfectly established the expected I-V development is appropriate, dependable, and suitable for analyzing of RS (Fig. 8 and Table 5).

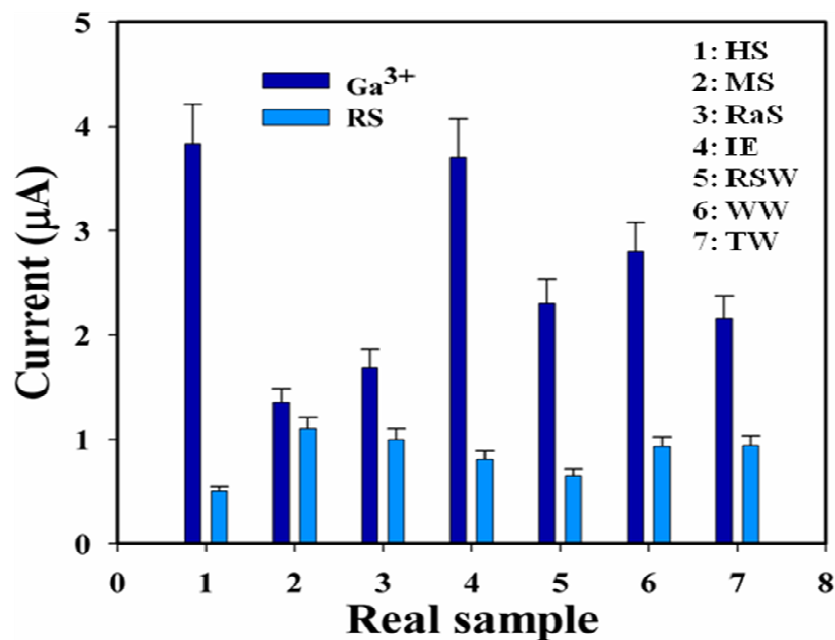


Fig. 8 Real sample examination with the modified electrodes

Table 5. Real sample analyses

ME	AC, Ga ³⁺ (25 µL, µM)	OC, Ga ³⁺ (µA)	RSA (25 µL)	ROC (RSA, µA)				FC (µM)	R (%)	SD (n = 3)	RSD (%) n = 3
				R1	R2	R3	A				
1	1.0	3.83	HS	2.32	1.82	1.60	1.92	0.50	50	0.37	19.28
2	1.0	1.35	MS	1.47	1.55	1.45	1.49	1.10	110	0.05	3.55
3	1.0	1.69	RaS	1.82	1.66	1.60	1.70	1.0	101	0.11	6.72
4	1.0	3.70	IE	3.58	2.69	2.77	3.01	0.81	81	0.49	16.34
5	1.0	2.30	RSW	1.88	1.35	1.27	1.50	0.65	65	0.33	22.10
6	1.0	2.80	WW	2.80	2.57	2.41	2.59	0.93	93	0.20	7.56
7	1.0	2.16	TW	2.43	1.99	1.64	2.02	0.94	94	0.40	19.60

ME: Modified electrode, AC: Added concentration, OC: Observed current, RSA: Real sample added, ROC: Respective observed current, R: Reading, A: Average, FC: Found concentration,

R: Recovery, *SD*: Standard deviation, *RSD*: Relative standard deviation, *HS*: Human serum, *U*: Urine, *IE*: Industrial effluent, *RSW*: Red sea water, *WW*: Well water, and *TW*: Tap water.

6. Conclusion

MBBSH molecules were synthesized using a simple condensation method, characterized, and used to detect poisonous heavy metal ion using current-voltage (I-V) procedure. Good performances of Ga^{3+} sensor was evaluated in points of sensitivity, LOD, LOQ, LDR, response time, reproducible, and repeatability predisposition. The 4-MBBSH/GCE sensor exhibited analytical performances with good results such as sensitivity ($949.37 \text{ pA}\mu\text{M}^{-1}\text{cm}^{-2}$), LOD ($\approx 84.0 \pm 0.2 \text{ pM}$), LOQ ($280.0 \pm 0.5 \text{ mM}$), LDR ($100.0 \text{ pM} \sim 1.0 \text{ mM}$), and response time (7.0 s) towards Ga^{3+} . This novel innovation can be established as an investigative tool for superior selectivity and quick detection of gallium ion using 4-MBBSH modified GCE with a nafion matrix. An inventive development can be introduced from this narrative approach for the monitoring of toxic HMI in health care and ecological arena.

Acknowledgement

Center of Excellence for Advanced Materials Research (CEAMR), Chemistry Department, King Abdulaziz University, Jeddah is acknowledged for instrumental, and technical support.

Associated content: ORCID

Mohammad Musarraf Hussain: 0000-0001-9270-0474

Mohammed M. Rahman: 0000-0003-2773-1244

References

1. M. M. Hussain, M. M. Rahman, and A. M. Asiri, *J. Environ. Sci.*, 2017, **53**, 27.
2. M. M. Rahman, M. M. Hussain, and A. M. Asiri, *RSC Adv.*, 2016, **6**, 65338.
3. M. M. Rahman, M. M. Hussain, and A. M. Asiri, *New J. Chem.*, 2017, **41**, 6667.
4. M. M. Hussain, M. M. Rahman, and A. M. Asiri, *PLOS ONE* 2016, **11**, e0166265.
5. M. M. Rhaman, M. M. Hussain, and A. M. Asiri, *Microchim. Acta* 2016, **183**, 3255.
6. M. M. Hussain, M. M. Rhaman, and A. M. Asiri, *Microchim. Acta* 2016, **183**, 3265.
7. M. M. Hussain, M. M. Rahman, A. M. Asiri, and M. R. Awual, *RSC Adv.*, 2016, **6**, 80511.
8. F. A. de Santana, J. T. P. Barbosa, G. D. Matos, M. G. A. Korn, and S. L. C, Ferreira, *Microchem. J.*, 2013, **110**, 198.
9. A. N. Anthemidis, G. A. Zachariadis, and J. A. Stratis, *Talanta*, 2003, **60**, 929.
10. V. K. Singh, N. K. Agnihotri, H. B. Singh, and R. L. Sharma, *Talanta*, 2001, **55**, 799.
11. M. J. G. Gonzalez, O. D. Renedo, M. A. A. Lomillo, and M. J. A, *Talanta*, 2004, **62**, 457.
12. S. K, *Anal. Chim. Acta*, 2006, **562**, 204.
13. H. S. Sharma, T. K. Bhardwaj, P. C. Jain, and S. K, *Talanta*, 2007, **71**, 1263.
14. T. H. A. Hasanin, Y. Okamoto, and T. Fujiwara, *Talanta*, 2016, **148**, 700.
15. C-C. Wu, and H-M. Liu, *J. Hazardous Mater.*, 2009, **163**, 1239.
16. M. M. Rhaman, M. M. Hussain, and A. M. Asiri, *PLOS ONE*, 2017, **12**, e0177817.
17. M. M. Rhaman, M. M. Hussain, and A.M. Asiri, *Progress Nat. Sci. Mater. Intl.*, 2017, **27**, 566.
18. B-Y. Kim, H-S. Kim, and A. Helal, *Sens. Actuators B* 2015, **206**, 430.
19. Agilent Crys, Yarnton, England, 2012.

20. G. M. Sheldrick, *Acta Cryst.*, 2008, **A64**, 112.
21. A. L. Spek, Utrecht University, Utrecht, 2005.
22. L. J. Farrugia, *J. Appl. Cryst.*, 1999, **32**, 837.
23. L. J. Farrugia, *J. Appl. Cryst.*, 2012, **45**, 849.
24. O. V. Dolomanov, L. J. Bourhis, R. J. Gildea, J. A. K. Howard, and H. Puschmann, *J. Appl. Cryst.*, 2009, **42**, 339.
25. M. M. Hussain, M. M. Rahman, M. N. Arshad, and A. M. Asiri, *ACS Omega*, 2017, **2**, 420.
26. M. N. Arshad, O. Sahin, M. Zia-ur-Rahman, I. U. Khan, A. M. Asiri, and H. M. Rafique, *J. Struct. Chem.*, 2013, **54**, 437.
27. M. N. Arshad, O. Sahin, M. Zia-ur-Rehman, M. Shafiq, I. U. Khan, A. M. Asiri, S. B. Khan, and K. A. Alamry, *J. Chem. Cryst.*, 2013, **43**, 671.
28. M. N. Arshad, T. Mahmood, A. F. Khan, M. Zia-Ur-Rehman, A. M. Asiri, I. U. Khan, R. Un-Nisa, K. Ayub, A. Mukhtar, and M. T. Saeed, *Chinese J. Struct. Chem.*, 2015, **34**, 15.
29. M. Shafiq, I. U. Khan, M. Zia-Ur-Rehman, M. N. Asghar, A. M. Asiri, and M. N. Arshad, *Asian J. Chem.*, 2012, **24**, 4799.
30. J. Bernstein, R. E. Davis, L. Shimoni, and N.-L. Chang. *Angew. Chem. Int. Ed. Engl.*, 1995, **34**, 1555.
31. M. R. Cunha, M. T. Tavares, C. F. Carvalho, N. A. T. Silva, A. D. F. Souza, G. J. V. Pereira, F. F. Ferreira, and R. P-Filho, *ACS Sustainable Chem. Eng.*, 2016, **4**, 1899.
32. A. A. Hummer, A. Rompel, *Metallomics*, 2013, **5**, 597.
33. L. R. Bernstein, T. Tanner, C. Godfrey, B. Noll, *Metal-Based Drugs*, 2000, **7**, 33.
34. M. M. Hussain, M. M. Rahman, M. N. Arshad, and A. M. Asiri, *Sci. Rep.*, 2017, **7**, 5832.

35. M. M. Hussain, M. M. Rahman, M. N. Arshad, and A. M. Asiri, *ChemistrySelect*, 2017, **2**, 7455-7464.
36. J. V. Kamat, S. K. Guin, J. S. Pillai, and S. K., *Talanta*, 2011, **86**, 256.
37. H. Filik, M. Dogutan, E. Tutem, and R. Apak, *Anal. Sci.*, 2002, **18**, 955.
38. N. Scott, D. E. Carter, and Q. Fernando, *Anal. Chem.*, 1987, **59**, 888.
39. D. Kara, A. Fisher, M. Foulkes, and S. J. Hill, *Spectrochim. Acta A: Molecul. Biomolecul. Spectros.*, 2010, **75**, 361.
40. M. S. Gidwani, S. K. Menon, and Y. K. Agrawal, *React. Funct. Polym.*, 2002, **53**, 143.
41. H. Kawaguchi, T. Shimizu, T. Shirakashi, and Y. Shijo, *Bull. Chem. Soc. Jpn.*, 1998, **71**, 647.
42. M. Kumar, M. Mohapatra, P. J. Purohit, S. K. Thulasidas, T. K. Seshagiri, N. Goyal, and S. V. Godbole, *At. Spectros.*, 2010, **31**, 97.
43. R. M. Argollo, and J-G. Schilling, *Anal. Chim. Acta*, 1978, **96**, 117.
44. D. G. Filatova, I. F. Seregina, L. S. Foteeva, V. V. Pukhov, A. R. Timerbaev, and M. A. Bolshov, *Anal. Bioanal. Chem.*, 2011, **400**, 709.
45. K. J. Orians, and E. A. Boyle, *Anal. Chim. Acta*, 1993, **282**, 63.
46. J. Wang, and J. M. Zadeii, *Anal. Chim. Acta*, 1986, **185**, 229.
47. R. Piech, *Electroanal.*, 2009, **21**, 1842.
48. A. Abbaspour, S. M. Khosfetrat, H. Sharghi, and R. Khalifeh, *J. Hazard. Mater.*, 2011, **185**, 101.
49. B. Tang, Z-Z. Chen, N. Zhang, J. Zhang, and Y. Wang, *Talanta*, 2006, **68**, 575.